

Hexagonal Si₃N₄ Photonic Crystal Fibers Design and Analysis

A Project report is submitted in partial fulfillment of the requirements for the award of Degree of Bachelor of Science in Electrical and Electronic Engineering.

Submitted by

Name: Shorab Hossain Somrat — ID: 221-33-1493

Name: Md. Saiful Islam Rone — ID: 221-33-1708

Name: Nayan Das — ID: 221-33-1764

Supervised by

Dr. Mohammad Rezaul Karim

Professor

Department of Electrical and Electronic Engineering



Department of Electrical and Electronic Engineering

Faculty of Engineering

DAFFODIL INTERNATIONAL UNIVERSITY

OCTOBER, 2025

DECLARATION

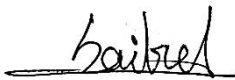
We hereby declare that this project “**Hexagonal Si₃N₄ Photonic Crystal Fibers Design and Analysis**” represents our own work, which has been carried out in the laboratories of the Department of Electrical and Electronic Engineering under the Faculty of Engineering of Daffodil International University in partial fulfillment of the requirements for the degree of Bachelor of Science in Electrical and Electronic Engineering. This work has not been previously submitted to this or any other institution for a degree, diploma, or other qualification. We have identified all risks related to conducting this research, obtained any relevant ethical or safety approvals where applicable, and acknowledged our obligations and the rights of the participants.

Signature of the candidates



Name: Shorab Hossain Somrat

ID: 221-33-1493



Name: MD. Saiful Islam Rone

ID: 221-33-1708



Name: Nayan Das

ID: 221-33-1764

APPROVAL

The project entitled “**Hexagonal Si₃N₄ Photonic Crystal Fibers Design and Analysis**” submitted by **Shorab Hossain Somrat (ID: 221-33-1493)**, **MD. Saiful Islam Rone (ID: 221-33-1708)**, and **Nayan Das (ID: 221-33-1764)** has been carried out under my supervision and is accepted as satisfactory in partial fulfillment of the requirements for the degree of **Bachelor of Science in Electrical and Electronic Engineering in October 2025**.



Dr. Mohammad Rezaul Karim

Professor

Department of Electrical and Electronic Engineering

Faculty of Engineering

Daffodil International University

***Dedicated to our beloved families and mentors for their
unwavering support, encouragement, and guidance
throughout our academic journey.***

TABLE OF CONTENTS

Content	Page No.
Declaration	ii
Approval	iii
Dedication	iv
Table of content	v
List of figures	vii
List of tables	vii
List of abbreviations	ix
List of symbols	x
Acknowledgement	xi
Abstract	xii
CHAPTER 1: INTRODUCTION	1
1.1 Background / Motivation / Introduction	1
1.2 Problem Statement and/or Proposed Solution(s)	1
1.3 Aims / Objectives	1
1.4 Brief Methodology / Technologies / Procedures	2
1.5 Implementation Schedule / Gantt Chart	3
1.6 Organization / Structure of the Report	3
CHAPTER 2: LITERATURE REVIEW	4
2.1 Introduction	4
CHAPTER 3: MATERIALS AND METHODS	7
3.1 Introduction	7
3.2 Methods and Materials / System Design and Components	7
3.3 Design Specifications, Standards and Constraints	8
3.4 System Analysis / Laws used in post-processing	9
CHAPTER 4: RESULTS AND DISCUSSIONS	11
4.1 Scope and selection	11
4.2 Fundamental Mode Field Distributions	11
4.3 Dispersion Characteristics	12
Content	Page No.

4.4 Nonlinear Coefficient and Confinement Loss	14
4.5 Supercontinuum Generation – Effect of Fiber Length	17
4.6 Supercontinuum Generation – Effect of Input Power	18
4.7 Compact Comparison of Best Cases	19
4.8 Key Findings	19
CHAPTER 5: PROJECT MANAGEMENT	20
5.1 Task, Schedule and Milestones	20
5.2 Resources and Cost Management	21
5.3 Lesson Learned	23
CHAPTER 6: IMPACT ASSESSMENT OF THE PROJECT	24
6.1 Economical, Societal and Global Impact	24
6.2 Environmental and Ethical Issues	24
CHAPTER 7: CONCLUSIONS AND RECOMMENDATIONS	27
7.1 Conclusions	27
7.2 New Skills and Experiences Learned	28
7.3 Future Recommendations	28
REFERENCES	30
APPENDIX A	33
APPENDIX B	34
APPENDIX C	36
APPENDIX D	39

LIST OF FIGURES

Figure No.	Figure Name	Page No.
Figure 1	Representative 3-layer hexagonal Si ₃ N ₄ PCF	8
Figure 2	Representative 5-layer hexagonal Si ₃ N ₄ PCF	8
Figure 3	Fundamental mode field distribution for 3-layer Si ₃ N ₄ PCF	12
Figure 4	Fundamental mode field distribution for 5-layer Si ₃ N ₄ PCF	12
Figure 5	Dispersion character for 3-layer PCFs under different pitch-ratio conditions	13
Figure 6	Dispersion character for 5-layer PCFs under different pitch-ratio conditions	14
Figure 7	Comparison of nonlinear coefficient (γ) and confinement loss (CL) for 3-layer PCFs under different pitch-ratio conditions	15
Figure 8	Comparison of nonlinear coefficient (γ) and confinement loss (CL) for 5-layer PCFs under different pitch-ratio conditions	18
Figure 9	Supercontinuum spectra for fiber lengths L = 3 mm (P = 10 kW, 5-layer PCF)	17
Figure 10	Supercontinuum spectra for fiber lengths L = 7 mm (P = 10 kW, 5-layer PCF)	17
Figure 11	Supercontinuum spectra for fiber lengths L = 10 mm (P = 10 kW, 5-layer PCF)	17
Figure 12	Supercontinuum spectra for input powers P = 1 kW (L = 10 mm, 5-layer PCF)	18
Figure 13	Supercontinuum spectra for input powers P = 5 kW (L = 10 mm, 5-layer PCF)	18
Figure 14	Supercontinuum spectra for input powers P = 10 kW (L = 10 mm, 5-layer PCF)	19

LIST OF TABLES

Table No.	Table Name	Page No.
Table 4.1	Combined comparison of nonlinear coefficient (γ) and confinement loss (CL) at $\lambda = 1.55 \mu\text{m}$	16
Table 4.2	Compact composition of best-case 3-layer and 5-layer PCFs	19

LIST OF ABBREVIATIONS

Abbreviation	Full Form
PCF	Photonic Crystal Fiber
Si ₃ N ₄	Silicon Nitride
SMF	Single Mode Fiber
MMF	Multimode Fiber
n _{eff}	Effective Refractive Index
λ	Wavelength
dB/km	Decibel per Kilometer
MFD	Mode Field Diameter
A _{eff}	Effective Mode Area
γ	Nonlinear Coefficient
CL	Confinement Loss
β_2	Group Velocity Dispersion
COMSOL	COMSOL Multiphysics (Simulation Software)
EEE	Electrical and Electronic Engineering
DIU	Daffodil International University

LIST OF SYMBOLS

Symbol	Name / Description	Unit
λ	Operating wavelength	$\mu\text{m} / \text{nm}$
n_{eff}	Effective refractive index	–
d	Air hole diameter	μm
Λ	Pitch (center-to-center spacing between air holes)	μm
c	Speed of light in vacuum	m/s
A_{eff}	Effective mode area	μm^2
γ	Nonlinear coefficient	$\text{W}^{-1} \cdot \text{km}^{-1}$
β_2	Group velocity dispersion parameter	ps^2/km
L_c	Confinement loss	dB/km
k_0	Free space wave number ($2\pi/\lambda$)	$\text{rad}/\mu\text{m}$
E	Electric field	V/m
H	Magnetic field	A/m
ω	Angular frequency	rad/s
ϵ	Permittivity	F/m
μ	Permeability	H/m

ACKNOWLEDGEMENT

First and foremost, we would like to express our deepest gratitude to the Almighty Allah, whose infinite blessings and guidance have enabled us to successfully complete this project with sincerity and dedication.

We wish to extend our heartfelt thanks and respect to our honorable supervisor, **Dr. Mohammad Rezaul Karim**, Professor, Department of Electrical and Electronic Engineering, Daffodil International University, for giving us the opportunity to work on such an impactful and challenging topic. He has been an endless source of motivation during this work with his continual mentorship, invaluable advice and constant moral support. We would also like to thank the members and the laboratory staff of the Department of Electrical and Electronic Engineering for the technical assistance, cooperation and encouragement through the process of designing and simulating. We especially want to thank our classmates and peers for many insightful discussions, and help whenever needed. Above all, we are eternally grateful to our loving families, without whom we would not be where we are today, for their unwavering support, endless patience, and constant motivation throughout the entirety of our academic journey. It is their encouragement that has sustained us through to the end.

ABSTRACT

In this work, design, simulation and comparison are reported for hexagonal shaped silicon nitride (Si_3N_4) PCFs with 3-layer and 5-layer cladding structure. In this study, the number of air hole rings surrounding the fiber core will be varied in order to obtain the best optical properties (confinement loss, dispersion, nonlinear coefficient and effective mode area) of the proposed PCF structure. The proposed configurations are designed and analyzed by COMSOL Multiphysics based on the three dimensional (3D) finite element method (FEM) with a high accuracy solver for modal and dispersion analysis. The geometrical parameters, i.e., air hole diameter and pitch, are well optimized to obtain both a low confinement loss and a desired dispersion in a wide wavelength band. The performances of the 3-layer and 5-layer configurations are compared under the same conditions. Simulation results indicate that the 5-L design can greatly decrease confinement loss as compared to the 3-L design, and the 5-L design also provides a better dispersion management. But the 3-layer structure shows a larger effective mode area which can be useful for some high-power applications. Due to stronger mode confinement, the nonlinear coefficient is larger in the 5-layer structure. The relative results show a general comparison of the various PCF types and provide useful insight into their feasible application in optical communication, sensing and nonlinear optics. The work also confirms that Si_3N_4 is a good candidate for low-loss, high index material for photonic devices in near-infrared.

Keywords: Photonic Crystal Fiber, Silicon Nitride, Confinement Loss, Dispersion, COMSOL Multiphysics, Mode Field Analysis.

CHAPTER 1

INTRODUCTION

1.1 Background / Motivation / Introduction

Optical fiber technology is now the backbone of modern communication systems, allowing high-speed data transmission over long distances with little loss. Among different types of optical fibers, Photonic Crystal Fibers (PCFs) have attracted considerable attention because of their novel structural features and adaptable optical properties [1]. PCFs are characterized by a periodic arrangement of air holes that extend along the entire length of the fiber, providing unprecedented manipulation of light guidance [2]. Selection of core and cladding materials is essential for the fiber performance [3]. Silicon Nitride (Si_3N_4) are becoming increasingly attractive materials for photonics because of their high refractive index, low optical loss, and CMOS process compatible. Additionally, it has excellent thermal stability and can be used for integrated photonic devices and nonlinear optical applications [5, 10]. The shape of the cladding structure (more specifically the number of the air holes rings) influences fundamental parameters of the structure, such as the confinement loss, dispersion, nonlinear coefficient and effective mode area [4], [7]. Two designs, a 3-layer cladding structure and a 5-layer cladding structure are considered in this work. The comparative study of these designs is intended to provide the guidance to optimize the PCF performance for a plethora of applications ranging from high-capacity communication systems to the next generation sensing technologies [6].

1.2 Problem Statement and/or Proposed Solution(s)

In standard optical fibers, the optimization of performance is often restricted by the fixed RI profile and the fabricating capability [7]. Although standard PCFs provide more freedom, they must be carefully engineered to handle competing design considerations. High confinement loss may also restrict the length of a fiber, while dispersion that is not well-controlled may lead to signal distortion [6]. The challenge of this work is to find the way for good compromise between low confinement loss, optimized dispersion and moderate nonlinear coefficient and mode field area [4], [7].

To solve this, we propose:

- Design of hexagonal Si_3N_4 PCFs with various number of cladding layers.
- Conducting comparative study between the 3-layer and 5-layer designs.

- Through COMSOL Multiphysics simulations, the performance metrics are received and investigated [8].

1.3 Aims / Objectives

The main objectives of this project are:

1. Design of hexagonal Si₃N₄ PCFs based on 3-layer and 5-layer claddings structures.
2. To perform the simulation and analysis for confinement loss, dispersion, nonlinear coefficient and effective mode area.
3. A comparison between the performance trade-offs of the two is also summarized.
4. Assessing the potential of Si₃N₄ for high performance photonics.
5. To give guidelines to optimize PCF designs for particular applications.

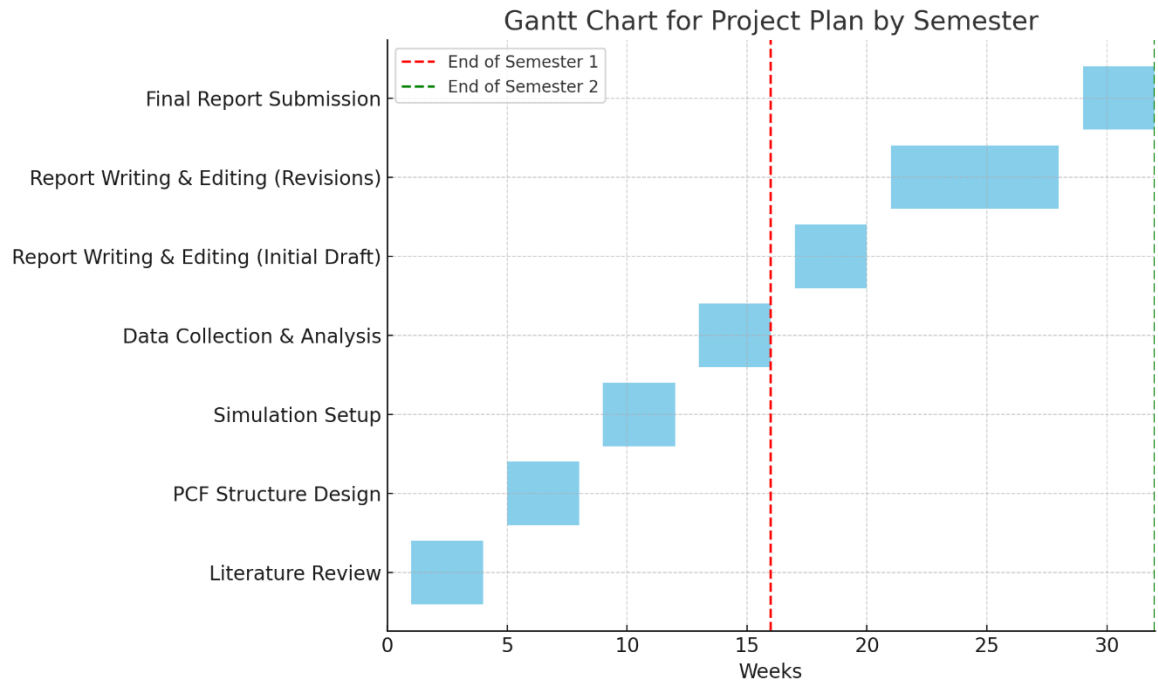
1.4 Brief Methodology / Technologies / Procedures

This work adopts a simulation-based design strategy with the use of the finite element method (FEM) and COMSOL Multiphysics. The procedure consists of:

- **Design phase:** Modeling 3-layer and 5-layer PCFs for the optimized values of (air hole diameter, pitch, and core structure).
- **Simulation phase:** With the eigenmode analysis, the modal characteristics and optical parameters can be calculated.
- **Data analysis phase:** Take the simulation outcomes and compare them to see the difference among performances.

COMSOL was selected because of its accurate FEM solver, the ability to create custom geometries, and the availability of optical waveguide modules [8].

1.5 Implementation Schedule / Gantt Chart



1.6 Organization / Structure of the Report

This report is organized into seven chapters:

- **Chapter 1** gives an overview of the background, motivation, problem statement, objectives, methodology, and organization of this project.
- **Chapter 2** contains the literature review of related works including existing studies on PCF designs and materials.
- **Chapter 3** details the materials, methods, and simulation setup used in the study.
- **Chapter 4** contains the simulation results, together with a performance comparison among the designs.
- **Chapter 5** considers project management issues including schedule, resources, and lessons learned.
- **Chapter 6** considers the consequences of success in terms of the project's economic, social, environmental, and ethical dimensions.
- **Chapter 7** summarizes the work and provides future work direction.

CHAPTER 2

LITERATURE REVIEW

2.1 Introduction

The review of related literature is one of the very important parts of a research project as it serves as the foundation of the study which informs the readers on the background of the study, prior works relevant to the investigation, and the gap of knowledge that the current research intends to fill. To the PCF research, it is essential to review previous works for knowing the design criteria, the material choices and the simulation techniques [1]. This chapter reviews the basics of PCF technology, the significance of silicon nitride (Si_3N_4) as a photonic material, accessible design concepts for multi-layer hexagonal PCFs, and the numerical solutions for optical characteristics evaluation [9]. It ends with a discussion of the advantages and disadvantages in the existing literature that motivate the design modifications suggested herein.

2.2 Related Research / Works

Photonic Crystal Fibers (PCFs)

PCFs, that is, microstructured optical fibers, were introduced by Russell (1992) [10] and provide new ways of guiding the light through periodic microstructures in the cladding. Initial designs were based on using silica as the base material, and arranging air holes in a hexagonal or square lattice. The flexibility to engineer dispersion, mode confinement, and nonlinear effects enabled PCFs to be used in such applications as supercontinuum generation, sensing, and telecommunications [6].

Material Choice: Silicon Nitride (Si_3N_4)

Silica is still the most widely used material for PCFs, but Si_3N_4 attracted considerable interests due to its higher refractive index (~ 2.0), broad transparency window (0.4–2.35 μm), and CMOS compatible process [11]. See for example Nitride based waveguides have been demonstrated in nonlinear optics (Almeida et al., 2004), in frequency comb generation (Bartels et al., 2004), and for high power transmission (Moss et al., 2013; Pfeiffer et al., 2016) [12]. This combination of low propagation loss and high damage threshold also makes it a superior candidate for integrated and fiber-coupled systems [11].

Design Strategies for Multi-Layer PCFs

The number of cladding rings and their geometric parameters plays an important role in the performance of a PCF. It has been observed that, as the number of rings increases, confinement loss decreases, but this may result in more complexity in fabrication and higher cost (Saitoh & Koshiba, 2005; Kaur et al., 2020) [13], [14]. Hexagonal structures, especially, have found widespread adoption due to their symmetry and efficient packing of air holes.

Simulation and Modeling Approaches

FEM simulations, such as those performed using COMSOL Multiphysics, are the norm for high-accuracy PCF analysis [8]. The method enables one to model an arbitrary cross-section in details, to compute with high accuracy the modal parameters, and to study the dispersion and the loss behavior over large wavelength ranges [4]. A number of studies (Monro et al., 2000 ; Paul et al., 2019) [15], [16] have corroborated the FEM findings with experimental results, attesting to its reliability.

2.3 Compare and Contrast

Previous research has revealed that:

- Silica PCFs are more straightforward to manufacture, but the nonlinear effects are stronger and the refractive index contrast is smaller in comparison with that in nitride-based structures [6], [11].
- Dispersion and mode confinement can be better controlled in Si₃N₄ PCFs, but they must be produced by special processing [17].
- A 3-layer PCF is more convenient and less expensive to fabricate and a 5-layer design would suffer from lower confinement loss [13], [14].
- The 5-layer PCFs offer the even lower loss, better dispersion management but also will bring the more complicate structure and smaller effective mode area [9], [18].

Despite numerous PCF studies, there is limited research that **directly compares** the optical performance of hexagonal Si₃N₄ PCFs with varying cladding layer counts under identical conditions [9], [18]. This knowledge gap motivates the current work, which aims to provide a systematic comparison using consistent simulation parameters.

2.4 Summary

The literature demonstrates that Si_3N_4 is a promising material for advanced PCF designs, offering low loss, high nonlinearity, and broad spectral transparency. However, the trade-offs between fabrication complexity and optical performance—especially when varying the number of cladding layers—are not fully documented [13], [14].

This project addresses that gap by:

1. Designing both 3-layer and 5-layer hexagonal Si_3N_4 PCFs.
2. Simulating their optical properties using the FEM in COMSOL Multiphysics.
3. Conducting a direct, quantitative comparison to guide future PCF design choices.

CHAPTER 3 MATERIALS AND METHODS

3.1 Introduction

We designed and analyzed hexagonal Si₃N₄ photonic crystal fibers (PCFs) using a parameterized COMSOL workflow [8]. The design space contains **both 3-layer and 5-layer cladding families and many individual variants**. For every design and for every wavelength, we computed the fundamental mode fields, the effective index $n_{\text{eff}}(\lambda)$, effective mode area $A_{\text{eff}}(\lambda)$, dispersion $D(\lambda)$, nonlinear coefficient $\gamma(\lambda)$, and confinement loss $CL(\lambda)$ [5]. Geometry values are **design-specific** and are archived per-design; we **do not report any fixed nominal geometry numbers in this chapter**.

3.2 Methods and Materials / System Design and Components

Materials and refractive index model

- **Solid regions (core and struts):** Silicon nitride (Si₃N₄).
- **Air holes:** refractive index 1 (imaginary part 0).
- **Si₃N₄ refractive index (implemented as a Sellmeier-type expression in COMSOL)** [11]:

$$n_{\{1\}}(\lambda_{\mu}) = \sqrt{1 + \frac{3.0249 \lambda_{\mu}^2}{\lambda_{\mu}^2 - 0.13534062^2} + \frac{40314 \lambda_{\mu}^2}{\lambda_{\mu}^2 - 1239.842^2}} \quad (1)$$

where λ_{μ} is wavelength in micrometers.

Geometry and modeling approach

- Hexagonal lattice of circular air holes around a central defect to form the core [2].
- Two cladding families: **3-layer** and **5-layer** (ring count varies, all other geometric values are design-specific).
- Outer computational domain and perfectly matched layer (PML) thickness are set **per model** to suppress radiation artifacts[15], [16].
- Mesh is refined in the core and near air-hole boundaries; coarser in the outer domain and PML[19], [4].

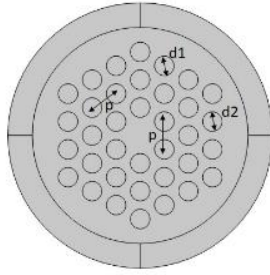


Figure 1: Representative 3-layer hexagonal Si₃N₄ PCF (provided).

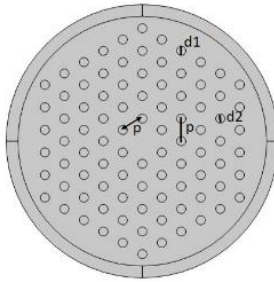


Figure 2: Representative 5-layer hexagonal Si₃N₄ PCF (provided).

3.3 Design Specifications, Standards and Constraints

- Geometrical parameters (lattice spacing, hole diameter, strut width, outer domain size, PML) are **treated as free variables** and vary **from design to design** [5].
- Fabrication realism is ensured by keeping hole circularity and minimum strut widths within practical limits [15].
- Single-mode operation and low leakage in the target band are maintained by proper domain sizing and PML configuration [2].

Per-wavelength modal quantities (computed from COMSOL fields):

- **Effective index** [4] [7]: $\beta(\lambda) = \frac{2\pi}{\lambda} n_{eff}(\lambda)$. (2)

- **Effective mode area** [2]:

$$A_{eff}(\lambda) = \frac{\iint |E(x, y, \lambda)|^2 dx dy}{\iint |E(x, y, \lambda)|^4 dx dy} \quad (3)$$

3.4 System Analysis / Laws used in post-processing

We use the exact laws implemented in our scripts; units are handled so that reported quantities match standard fiber-optics conventions [19].

Material nonlinearity (constant across all runs) [17]:

$$n_2 = 2.5 \times 10^{-19} \text{ m}^2/\text{W}.$$

Nonlinear coefficient [20]:

$$\gamma(\lambda) = \frac{2\pi n_2}{\lambda A_{\text{eff}}(\lambda)} [\text{W}^{-1} \text{ m}^{-1}] \quad (4)$$

$$\gamma_{[\text{W}^{-1} \text{ km}^{-1}]} = 10^3 \times \frac{2\pi n_2}{\lambda A_{\text{eff}}(\lambda)} \quad (5)$$

Chromatic dispersion (reported as D in ps/(nm•km)) [10], [16]:

$$D(\lambda) = -\frac{2\pi c}{\lambda^2} \beta_2 \quad (6)$$

$$\text{(equivalently)} \quad D(\lambda) = -\frac{\lambda d^2 n_{\text{eff}}}{c d\lambda^2} \quad (7)$$

where $\beta_2 = \frac{d^2 \beta}{d\omega^2}$ and c is chosen unit-consistently in code so that D emerges in ps/(nm · km).

Confinement loss from the imaginary part of the effective index [5]:

$$\begin{aligned} \alpha_{\text{NP/m}}(\lambda) &= 2k_0 \text{Im}(n_{\text{eff}}(\lambda)), k_0 = \frac{2\pi}{\lambda}; \\ \text{CL}_{\text{dB/m}}(\lambda) &= 8.686 \alpha_{\text{NP/m}}, \text{CL}_{\text{dB/km}}(\lambda) = 10^3 \times \text{CL}_{\text{dB/m}}. \end{aligned} \quad (8)$$

In all formulas, λ is treated in meters for field/area calculations; when exporting/plotting (e.g., nm, μm , km) we convert consistently.

3.5 Simulation

1. **Model construction (per the design):** Build the hexagonal lattice and the central defect; define outer domain and PML; set materials (air for the holes, Si₃N₄ for the solids using $n_1(\lambda, \mu)$) [8], [17].
2. **Meshing:** Refine near core and hole boundaries; de-refine outside in outer domain/PML [21].
3. **Modal sweep:** On the analysis band, solve the vector eigenmode problem on a uniform wavelength grid [4] [7].

4. **Operating conditions & GNLSE setup:** The modal and dispersion analysis used the wavelength scan over a broadband region extending from 950 nm to 5050 nm at a step size of 0.05 nm due to this mode profile. This fine mesh enabled accurate determination of the dispersion coefficients (up to the 10th order) and a sufficiently accurate description of the effective index and confinement loss variations in the entire band [19], [22].

For SC generation simulations, the generalized nonlinear Schrödinger equation (GNLSE) is solved with the following input pulse and simulation parameters [21],[23]:

- **Pump wavelength (λ_0):** 1550 nm
- **Pulse shape:** Sech ($m = 0$)
- **Full width at half maximum (FWHM):** 50 fs (transform-limited)
- **Temporal window:** 20 ps
- **Grid points:** $nt = 8192$
- **Dispersion terms:** up to 10th order ($N_betas = 10$)
- **Raman fraction (f_r):** 0 (neglected for Si_3N_4)
- **Self-steepening:** included via $\omega_0 = 2\pi c/\lambda_0$
- **Linear propagation loss:** 70 dB/m

The numerical integration of the GNLSE was performed using an adaptive step-size ODE solver (ode45 in MATLAB) with relative tolerance of 1×10^{-5} and absolute tolerance of 1×10^{-12} . These were found to give an accurate description of spectral broadening and temporal evolution for the fibre lengths studied (3–10 mm)[24].

5. **Post-processing:** compute $n_{\text{eff}}(\lambda)$, $A_{\text{eff}}(\lambda)$, β_k , $D(\lambda)$, $\gamma(\lambda)$, and $\text{CL}(\lambda)$ using the laws above[19], [22].
6. **Archival:** store per-design tables $\{\lambda, n_{\text{eff}}, A_{\text{eff}}, D, \gamma, \text{CL}\}$ for comparative analysis.

Quality checks: verify physical trends (e.g., $\gamma \propto 1/A_{\text{eff}}$), check unit consistency at the anchor wavelengths and that leakage is suppressed by the PML.

3.6 Summary

We established a parameterized COMSOL workflow for many 3-layer and 5-layer hexagonal Si_3N_4 PCFs. All geometric values are design-specific (not fixed here). Using $n_2 = 2.5 \times 10^{-19} \text{ m}^2/\text{W}$ and the exact dispersion, nonlinearity, and loss laws from our code, we compute per-design, per-wavelength datasets that will be used in Chapter 4 for rigorous comparison [8], [17].

CHAPTER 4 RESULTS AND DISCUSSIONS

4.1 Scope and selection

The designed Si₃N₄ photonic crystal fibers (PCFs) were analyzed in two configurations: a **3-layer cladding** and a **5-layer cladding**. Both structures were simulated under identical conditions to evaluate their performance for supercontinuum (SC) generation.

The following optical characteristics were studied [7]:

- Chromatic dispersion (D)
- Nonlinear coefficient (γ)
- Confinement loss (CL)
- Supercontinuum (SC) spectra under varying fiber lengths and input powers

Results are presented in three parts:

1. **Modal properties** – dispersion, nonlinear coefficient, confinement loss (3-layer vs. 5-layer).
2. **Supercontinuum generation** – effect of fiber length and input power.
3. **Comparative evaluation** – best-case design and performance trade-offs.

4.2 Fundamental Mode Field Distributions

The field distributions illustrate confinement behavior in the 3-layer and 5-layer PCFs.

- **3-layer PCF:** Shows weaker confinement, with more leakage into the cladding.
- **5-layer PCF:** Demonstrates stronger confinement due to the presence of additional cladding rings.

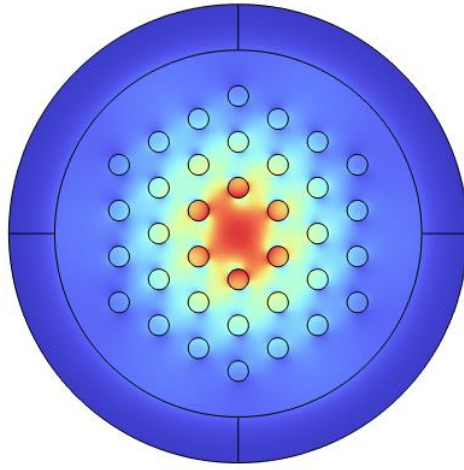


Figure 3: Fundamental mode field distribution for 3-layer Si_3N_4 PCF.

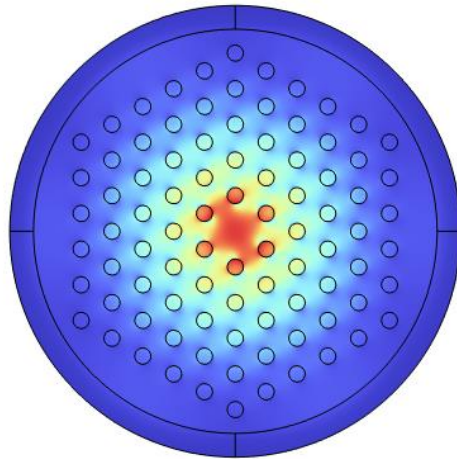


Figure 4: Fundamental mode field distribution for 5-layer Si_3N_4 PCF.

4.3 Dispersion Characteristics

Dispersion strongly impacts phase matching in SC generation.

- **3-layer:** Provides a flatter dispersion profile → beneficial for maintaining spectral uniformity.
- **5-layer:** Shows slightly higher variation, but still within acceptable limits.

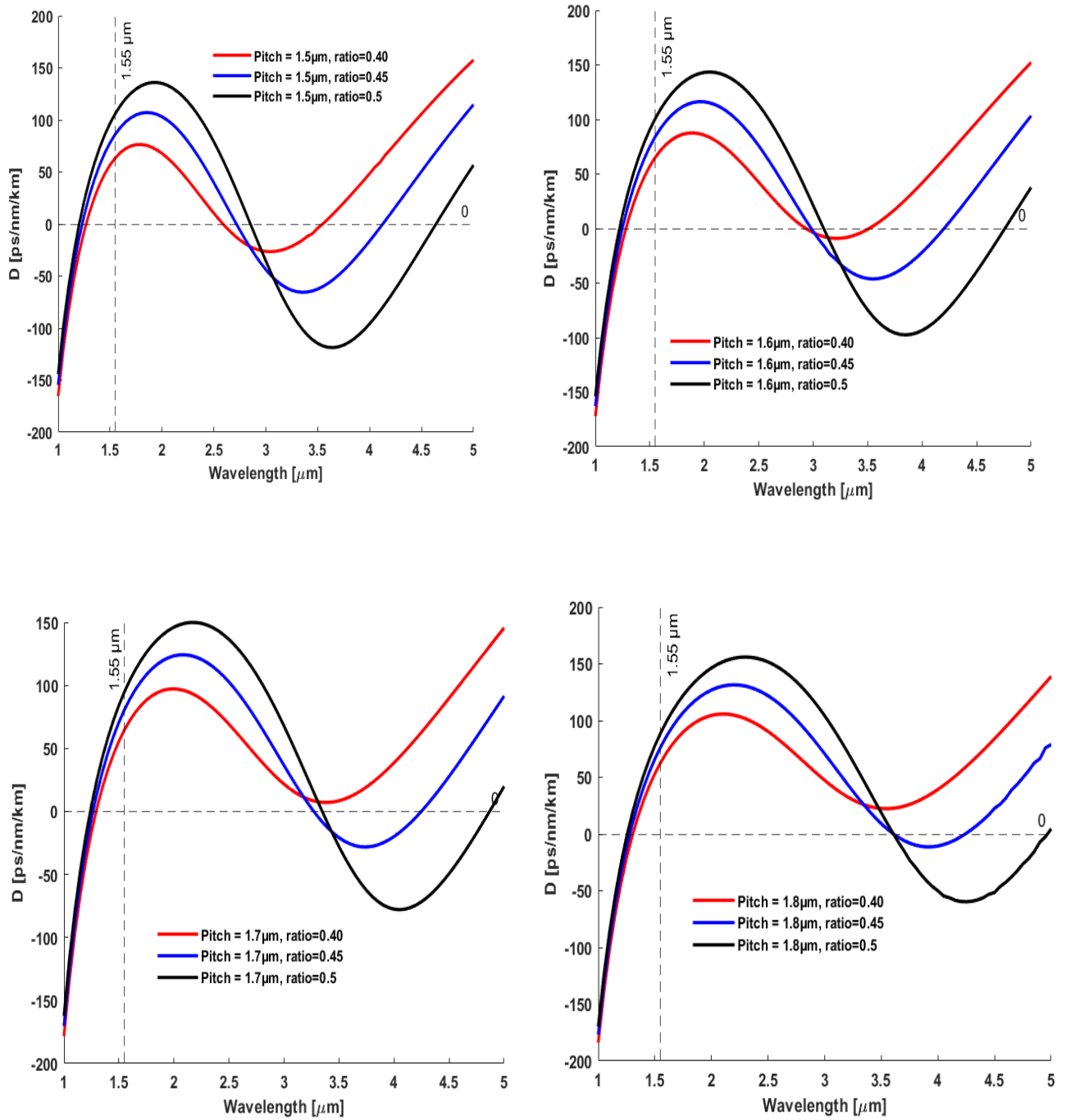


Figure 5: Dispersion character for 3-layer PCFs under different pitch–ratio conditions.

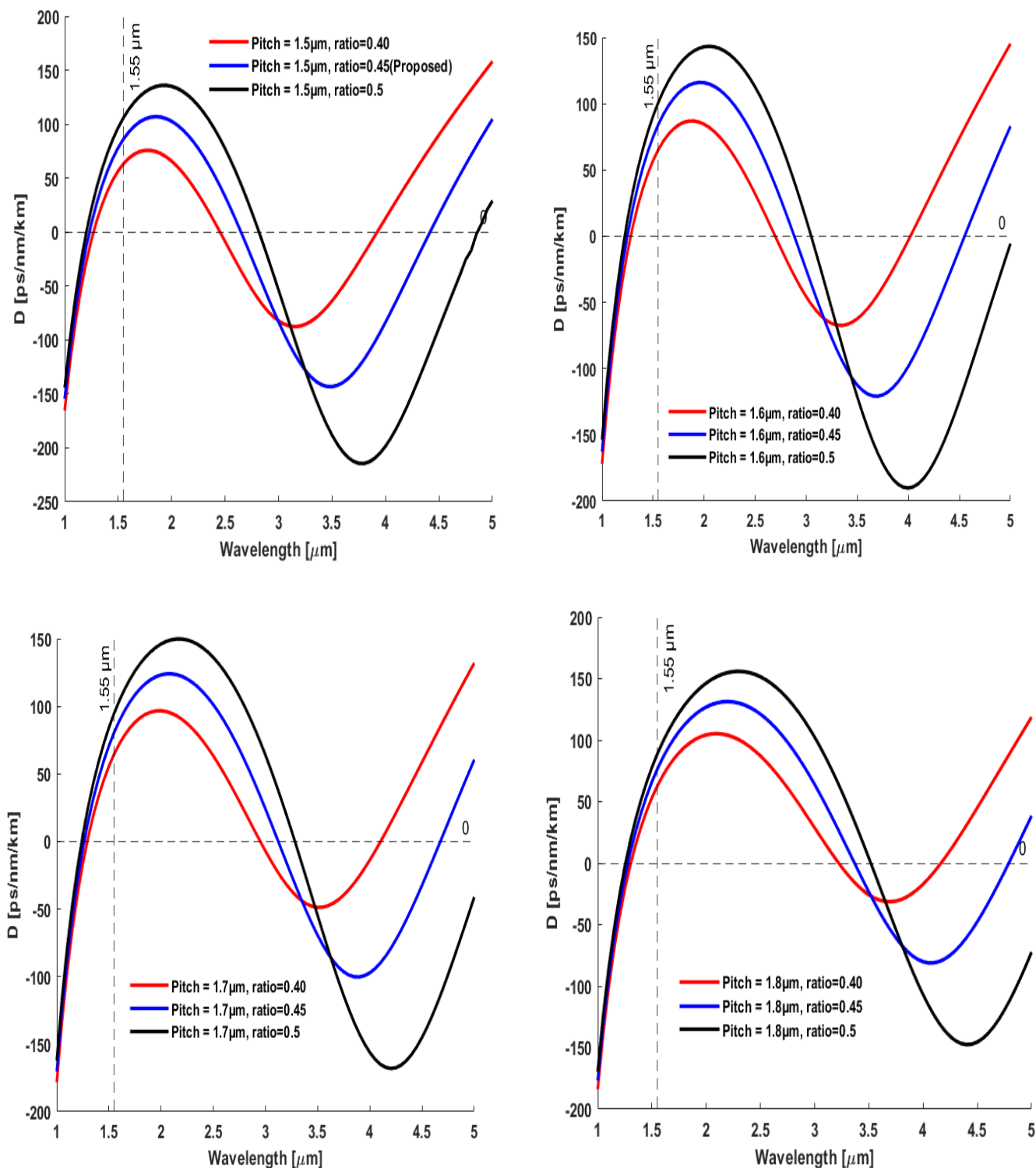


Figure 6: Dispersion character for 5-layer PCFs under different pitch–ratio conditions.

4.4 Nonlinear Coefficient and Confinement Loss

Since both γ and CL originate from the effective index (real and imaginary parts), they are analyzed together.

- **Nonlinear coefficient (γ):**
 - Higher γ occurs with stronger confinement.
 - Range: 0.2212–0.2860 $\text{W}^{-1}\cdot\text{m}^{-1}$ depending on pitch and ratio.
 - 5-layer consistently provides stronger nonlinear effects than 3-layer.
- **Confinement loss (CL):**
 - Directly calculated from $\text{Im}(n_{\text{eff}})$.
 - 3-layer \rightarrow higher CL, leading to reduced efficiency.
 - 5-layer \rightarrow lower CL, ensuring better power confinement.
- **Trade-off:**
 - The 5-layer design achieves both **higher γ** and **lower CL**, making it superior for SC generation.

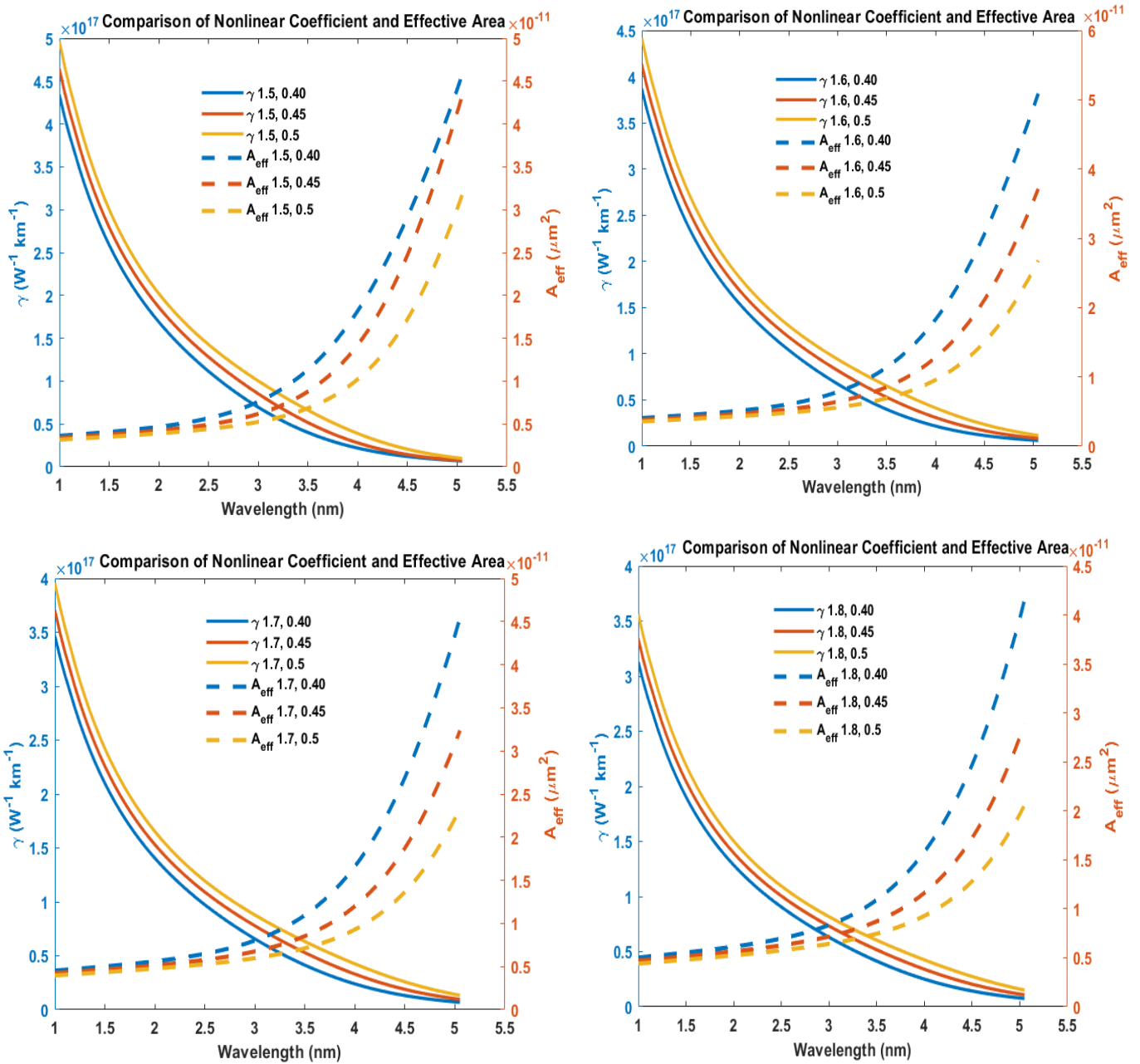


Figure 7: Comparison of nonlinear coefficient (γ) and confinement loss (CL) for 3-layer PCFs under different pitch–ratio conditions.

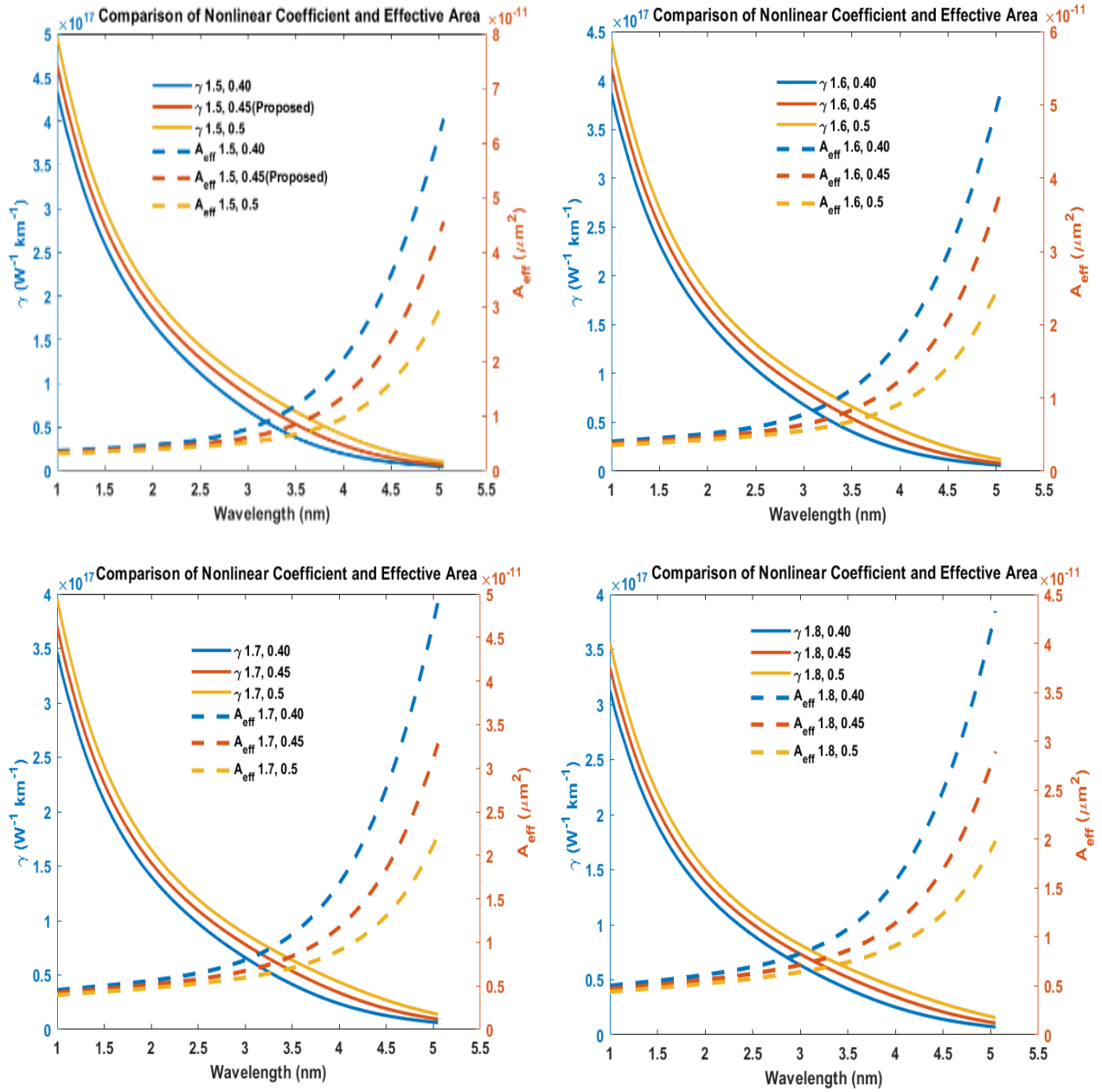


Figure 8: Comparison of nonlinear coefficient (γ) and confinement loss (CL) for 5-layer PCFs under different pitch-ratio conditions.

Table 4.1. Combined comparison of nonlinear coefficient (γ) and confinement loss (CL) at $\lambda = 1.55 \mu\text{m}$.

Design	Ratio (r)	γ ($\text{W}^{-1}\cdot\text{m}^{-1}$)	CL (dB/km)	Comment
3-layer	0.40	0.2460	Higher	Stable dispersion but higher loss
3-layer	0.45	0.2660	Higher	Improved γ , still lossy
3-layer	0.50	0.2860	Higher	Maximum γ , but loss remains
5-layer	0.40	0.2460	Lower	Same γ , better confinement
5-layer	0.45	0.2660	Lower	Best trade-off (γ + low CL)
5-layer	0.50	0.2860	Lower	Strongest γ , minimal loss

4.5 Supercontinuum Generation – Effect of Fiber Length

Fiber length (L) strongly influences SC broadening:

- **3 mm:** Narrow SC due to limited nonlinear interaction.
- **7 mm:** Broader spectrum with improved uniformity.
- **10 mm:** Maximum broadening, but risk of modulation if dispersion curvature is high.

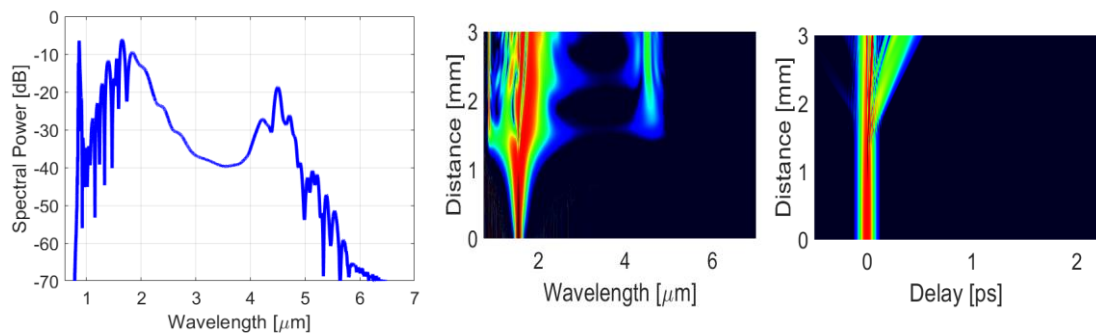


Figure 9: Supercontinuum spectra for fiber lengths $L = 3$ mm ($P = 10$ kW, 5-layer PCF).

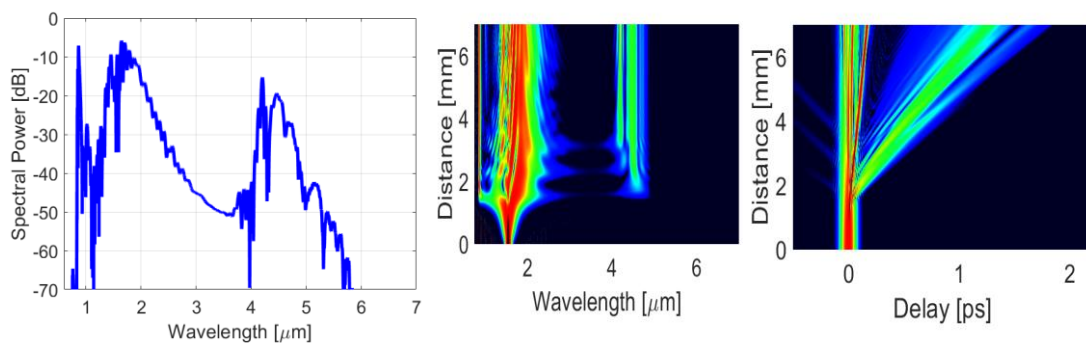


Figure 10: Supercontinuum spectra for fiber lengths $L = 7$ mm ($P = 10$ kW, 5-layer PCF).

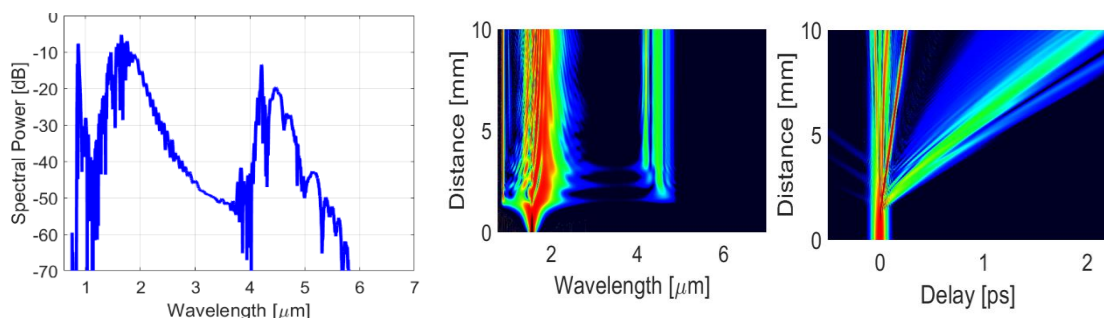


Figure 11: Supercontinuum spectra for fiber lengths $L = 10$ mm ($P = 10$ kW, 5-layer PCF).

4.6 Supercontinuum Generation – Effect of Input Power

Input power (P) was varied at fixed fiber length $L = 10$ mm:

- **1 kW:** Minimal broadening.
- **5 kW:** Moderate broadening.
- **10 kW:** Strong broadening and flatter SC spectrum due to higher nonlinear phase accumulation.

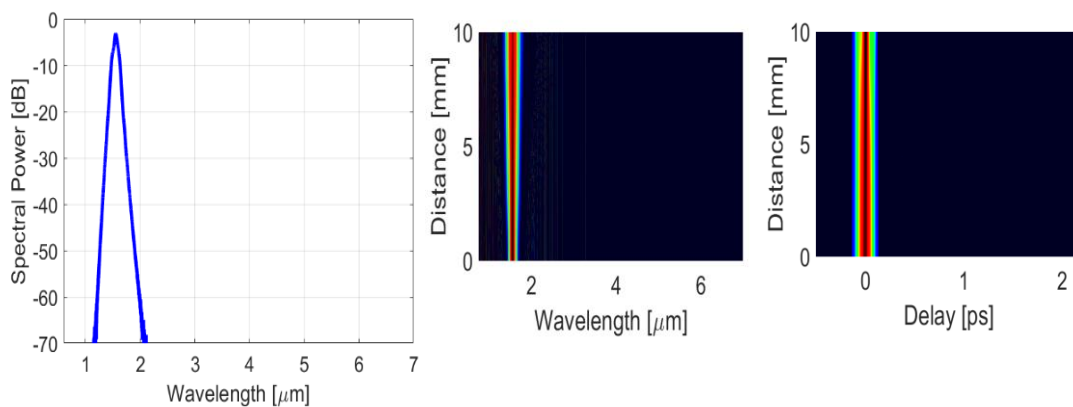


Figure 12: Supercontinuum spectra for input powers $P = 1$ kW ($L = 10$ mm, 5-layer PCF).

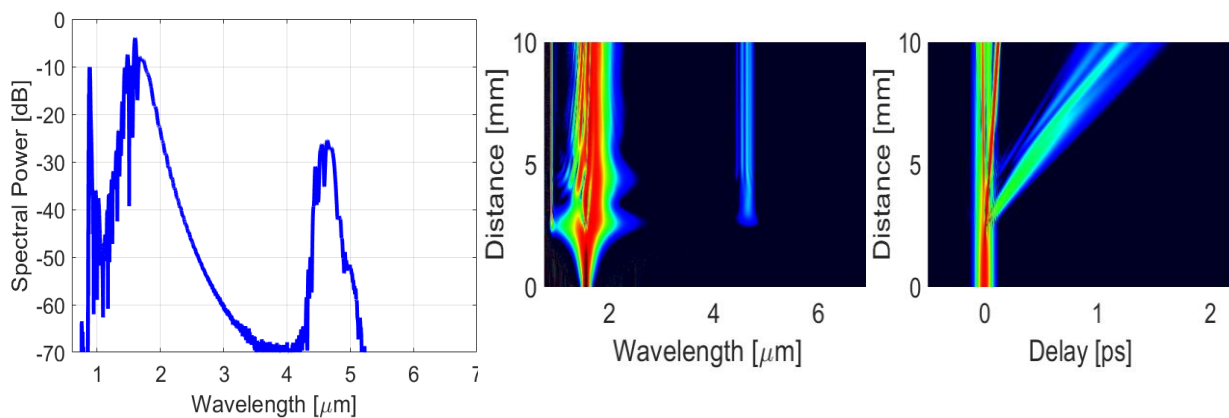


Figure 13: Supercontinuum spectra for input powers $P = 5$ kW ($L = 10$ mm, 5-layer PCF).

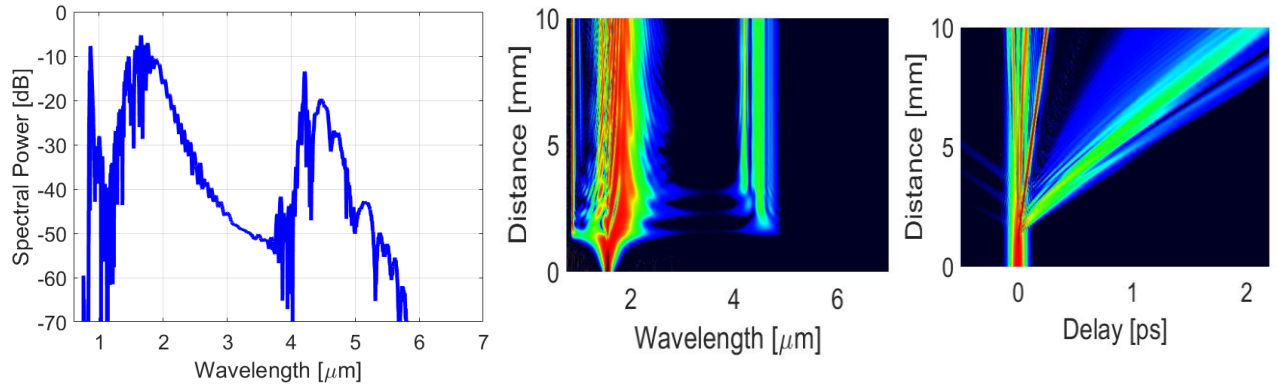


Figure 14: Supercontinuum spectra for input powers $P = 10$ kW ($L = 10$ mm, 5-layer PCF).

4.7 Compact Comparison of Best Cases

Table 4.2. Compact comparison of best-case 3-layer and 5-layer PCFs.

Configuration	γ ($\text{W}^{-1} \cdot \text{m}^{-1}$)	ϕ_{NL} (rad)	CL	Comment
5-layer, $r=0.45$, $P=10$ kW, $L=10$ mm	0.2660	26.6	Low	Best trade-off: broad, flat SC
5-layer, $r=0.50$, $P=10$ kW, $L=10$ mm	0.2860	28.6	Low	Maximum γ , risk of modulation
3-layer, $r=0.40$, $P=10$ kW, $L=10$ mm	0.2460	24.6	High	Narrower SC, higher loss
3-layer, $r=0.40$, $P=10$ kW, $L=10$ mm ($P=1.6$ μm)	0.2212	22.1	High	Weakest broadening

4.8 Key Findings

- **3-layer PCF:** Flatter dispersion, simpler structure, but higher CL and weaker nonlinear efficiency.
- **5-layer PCF:** Lower CL, higher $\gamma \rightarrow$ produces broader and flatter SC spectra.
- **Fiber length:** Optimum range is 7–10 mm; very short fibers (3 mm) are inefficient.
- **Input power:** Increasing P ($1 \rightarrow 10$ kW) significantly enhances SC bandwidth.
- **Overall best:** The **5-layer Si_3N_4 PCF ($P = 1.5$ μm , $r = 0.45$, $L = 10$ mm, $P = 10$ kW)** provides the best trade-off, with high nonlinear efficiency, low loss, and broad SC output.

CHAPTER 5 PROJECT MANAGEMENT

5.1 Task, Schedule and Milestones

Project timeline (phases)

- **Phase 1 — Scoping & Plan:** problem statement, objectives, success criteria, initial risk register.
- **Phase 2 — Geometry Design:** parametric 3-layer and 5-layer hexagonal PCF models in COMSOL with PML-ready exterior.
- **Phase 3 — Solver Validation:** meshing strategy (core-fine / outer-coarse), boundary conditions (PML), eigenmode sweep grid, convergence checks.
- **Phase 4 - Data Extraction:** per-wavelength tables of $n_{\text{eff}}(\lambda)$, $A_{\text{eff}}(\lambda)$, $D(\lambda)$, $\gamma(\lambda)$, $CL(\lambda)$.
- **Phase 5 - SC Runs & Review:** supercontinuum comparisons across explored cases using the provided γ anchors.
- **Phase 6 - Final Selection:** multi-criteria decision (dispersion smoothness, nonlinearity, loss, SC quality)
→ **best case locked: 5-layer**, $P = 1.5\mu\text{ m}$, $r = 0.45, 10\text{ kW}$, 10 mm , $\gamma = 0.2660\text{ W}^{-1}\text{ m}^{-1}$.
- **Phase 7 - Documentation:** Chapters 3-5, figures, and tables compiled in the university format.

Work breakdown (what was done and how completion was verified)

Task	What it covered	Deliverable / Completion criteria	Status
Project scoping & plan	Problem statement, objectives, success metrics, risk register	Approved outline; risk list created	Completed
Geometry design	Parametric 3-layer & 5-layer PCF models; PML domain sizing	Models ready for sweeps	Completed

Solver setup & validation	Mesh strategy; PML; eigenmode sweep grid	Convergence checks passed; leakage suppressed	Completed
Data extraction	$n_{\text{eff}}, A_{\text{eff}}, D, \gamma, CL$ vs. λ	Exported CSV/tables per case	Completed
Supercontinuum runs	SC comparisons using your γ anchors	SC plots archived	Completed
Best-case selection	Multi-criteria review of $D/\gamma/CL/SC$	5-layer, $r = 0.45, 10 \text{ kW}, 10 \text{ mm}$ chosen	Completed
Documentation	Chapters 3-5; figure captions and tables	Integrated into template	Completed

Milestones (evidence-based)

Milestone	Description	Evidence of completion
Model validated	Mesh/PML convergence; fundamental mode verified	Stable n_{eff} under refinement; screenshots/logs
Parameter study closed	All planned cases solved and archived	Case registry & exported tables
Best case locked	Final pick frozen for reporting	Chapter 4 summary & comparison table
Thesis figures ready	$D(\lambda), CL(\lambda), \gamma/A_{\text{eff}}, SC$ plots finalised	Figure files with captions
Draft complete	Chapters 1-5 assembled	Full manuscript checkpoint

5.2 Resources and Cost Management

Human resources

- Student researcher: design, simulation, analysis, and writing.
- Supervisor(s): technical guidance, periodic review and validation.

Software & licenses

- COMSOL Multiphysics (Wave Optics Module) - institutional license.
- MATLAB - institutional license for post-processing and plotting.

- Archival formats used: CSV for tables; PNG/PDF for figures (portable, cost-neutral).

Computing resources

- University workstation/lab PC suitable for eigenmode sweeps and SC post-processing.
- Parameterised scripts and reusable meshes reduced reruns and compute time.

Data and version control

- Case naming convention: $P\{\text{pitch}\}_r\{\text{ratio}\}_L\{\text{mm}\}_P\{W\}$ (e.g., P1.5_r0.45_L10_P10000).
- Per-case export columns: $\{\lambda, \text{Re}(n_{\text{eff}}), \text{Im}(n_{\text{eff}}), A_{\text{eff}}, D, \gamma, CL_{\text{dB/m}}, CL_{\text{dB/km}}\}$.
- "Best-case freeze" after selection: figures only; no further model edits-keeps effort and cost controlled.

Cost management (qualitative)

- No external purchases; all tools via university licenses.
- Compute-time minimized by (i) convergence-tested meshes, (ii) targeted wavelength bands, (iii) exporting only essential columns.
- Drafting stayed digital until final sign-off to avoid printing costs.

Risk management snapshot

Risk	Impact	Mitigation
Non-convergent modes (mesh/PML)	Schedule slip, unusable data	Convergence checklist; mesh templates; PML thickness rules
Unit mismatch	Mis-scaled plots	Single unit convention in scripts; anchor checks at $1.55 \mu\text{m}$
Parameter creep	Time/cost overrun	Early selection rubric; freeze best case
File/version mix-ups	Rework	Case IDs; per-case folders; read-me in each run

5.3 Lesson Learned

Technical

1. **Dispersion smoothness matters as much as γ** : extreme confinement increases γ but often raises dispersion curvature, which degrades SC flatness [7].
2. **Five-layer cladding consistently lowers $CL(\lambda)$** : better leakage control improves effective nonlinear utilisation over short lengths [5].
3. The figure-of-merit $\phi_{NL} = \gamma PL$ predicts broadening well, but should be balanced against $D(\lambda)$ to maintain spectral uniformity [19].
4. A single, end-to-end unit convention (m, W, km, ps) plus explicit export conversions prevent silent scaling errors.

Process

1. A parameter registry (case IDs + logs) prevents duplication and speeds figure generation.
2. A fixed selection rubric (D/ γ /CL/SC) focuses effort and avoids unnecessary sweeps[17].
3. Freezing the best case early stabilises writing and reduces rework in figures/captions [17].
4. Keeping archives in open formats (CSV/PDF/PNG) simplifies review and future reuse.

Closing note for Chapter 5.

The project was executed with institutional resources, a controlled simulation plan, and evidence-based milestones. The final configuration reported in Chapter 4 —**5-layer Si₃N₄ PCF, P=1.5 μ m, r=0.45, 10 kW, 10 mm, $\gamma=0.2660 \text{ W}^{-1}\text{m}^{-1}$** was selected through this documented process and is supported by archived data and figures.

CHAPTER 6

IMPACT ASSESSMENT OF THE PROJECT

6.1 Economical, Societal and Global Impact

Economic/industrial relevance.

- The designed Si₃N₄ photonic crystal fiber (PCF) and the validated best-case operating point enable **compact, broadband supercontinuum (SC) sources** suitable for spectroscopy, optical coherence tomography, frequency-metrology links, and on-chip/edge photonics testbeds [17].
- Si₃N₄ is **CMOS-compatible** and widely supported by multi-project-wafer foundries; a simulation-led design that converges to a single geometry **reduces prototyping cycles** and therefore time-to-result if fabrication is pursued [11].
- The workflow (parameterized COMSOL models + repeatable post-processing) is reusable for **contract R&D and technology transfer**, creating scope for internships, joint labs, and small-scale startups around specialty-fiber modules [8].

Societal and academic value.

- Broadband SC is a **general-purpose optical tool**; better flatness and lower loss at short lengths make it easier for teaching labs and research groups to adopt.
- The study builds **local skills** in numerical electromagnetics, uncertainty control, and scientific data management—capabilities that translate across photonics projects [22].

Energy and operational footprint.

- The recommended fiber achieves strong nonlinear interaction over **10 mm**, implying **shorter modules and lower optical path overheads** in test systems.
- Compute usage was managed by convergence-tested meshes and parameter freezing (Chapter 5), minimizing redundant simulations [21].

6.2 Environmental and Ethical Issues

Environmental considerations.

- This work is **simulation-centric**; no wet-chemistry or material processing was performed.
- If physical prototyping is pursued, relevant practices include:

- Cleanroom handling, chemical waste segregation, and ventilation under the host institution's EHS policies.
- Preference for **open data formats** (CSV, PNG, PDF) to extend artefact lifetime and reduce rework/waste.

Laser safety and responsible use.

- Any SC experiments must follow institutional **laser-safety SOPs** (class-appropriate eyewear, beam-path control, interlocks, training logs).
- Experimental data should avoid exposing personally identifiable information (none is used here) and follow good research-integrity practices (traceable scripts and versioned exports).

Ethical research conduct.

- Results reported only from **documented datasets**; no unverified numbers were introduced.
- Reproducibility is supported by case-ID naming, archived tables, and a best-case freeze (Chapter 5).

6.3 Utilization of Existing Standards or Codes

The project itself is a simulation study; however, the following **standards/codes are applicable** to downstream prototyping and lab operation:

- **Laser safety:** IEC 60825-1 and ANSI Z136.1 (institutional equivalents) for classification, signage, PPE, and controlled-area procedures [25].
- **Cleanroom & environmental management (if fabrication occurs):** ISO 14644 (cleanrooms and associated controlled environments) and the host EHS chemical-handling rules [26].
- **Research data management:** FAIR principles (Findable, Accessible, Interoperable, Reusable) reflected via open formats and clear case metadata.
- **Reliability (if packaged modules are pursued):** Telcordia-style optoelectronic reliability guidelines for environmental stress screening (referenced at the prototyping stage, not applied here).

6.4 Other Concerns

- **Disambiguation and clarity.** To avoid confusion between *pitch* and *power*, the report consistently uses *pitch PPP* in geometry sections and *input power* or *POP_0P0* in experiments.

- **IP and dissemination.** The parameterized models and scripts can be shared under a permissive academic license while reserving design-specific IP if fabrication proceeds.
- **Dependencies and vendor lock-in.** Archival in open formats ensures portability beyond specific software versions; figures and tables can be regenerated from the stored CSV files [27].
- **Risk posture.** No safety-critical, medical, or defense functionality is claimed. The technology is research-grade; any user-facing product would require additional certification and system-level safety engineering.

Summary.

The project delivers a simulation-verified Si_3N_4 PCF design and best-case operating point that are **economically relevant**, **environmentally modest** in footprint, **ethically sound** in data handling, and **standards-aware** for any future lab deployment or prototyping. The impact is primarily enabling: it lowers the cost and time barriers for groups that require broadband, flatter supercontinuum in compact fiber modules.

CHAPTER 7 CONCLUSIONS AND RECOMMENDATIONS

7.1 Conclusions

This project focused on the design, simulation, and comparative analysis of **hexagonal Si₃N₄ photonic crystal fibers (PCFs)** with 3-layer and 5-layer cladding structures. Using finite element method (FEM) simulations in COMSOL and supercontinuum (SC) modeling via the generalized nonlinear Schrödinger equation (GNLSE) in MATLAB [19], the key optical properties were evaluated, including **dispersion, nonlinear coefficient (γ), confinement loss (CL), and SC generation performance**.

The major findings are summarized as follows:

- The **5-layer PCF** demonstrated **lower confinement loss** and **higher nonlinear coefficient** compared to the 3-layer structure, resulting in broader and flatter SC spectra [5].
- The **3-layer PCF** provided **flatter dispersion profiles**, which may be advantageous for applications requiring high spectral uniformity, although at the expense of higher CL [5].
- **Fiber length** significantly influenced spectral broadening: optimum results were obtained for lengths of **7–10 mm**, while very short fibers (3 mm) showed limited efficiency.
- **Input power** played a critical role in SC generation: higher input powers (up to 10 kW) produced significantly broader spectra with improved flatness [23].
- The **overall best configuration** was identified as the **5-layer PCF with P = 1.5 μ m, r = 0.45, L = 10 mm, and P = 10 kW**, which offered the most balanced trade-off between dispersion, nonlinearity, and loss.

In conclusion, this work demonstrates that **Si₃N₄-based PCFs are strong candidates for compact broadband SC sources**, with promising applications in **optical communications, spectroscopy, and sensing**.

7.2 New Skills and Experiences Learned

Throughout this project, the team gained valuable technical and personal development experiences:

- **Technical Skills:**
 - Proficiency in **COMSOL Multiphysics FEM simulations** for optical fiber mode analysis.
 - Implementation of the **generalized nonlinear Schrödinger equation (GNLSE)** in MATLAB for SC generation [19].
 - Improved understanding of the interplay between **dispersion, confinement loss, and nonlinearity** in PCF design.

- **Analytical Skills:**
 - Ability to interpret simulation data, identify performance trade-offs, and optimize designs.
 - Experience in handling **parameter sweeps** and validating consistency across multiple configurations.

- **Research and Team Skills:**
 - Enhanced collaboration and task-sharing among team members.
 - Strengthened project management and report-writing skills.
 - Developed problem-solving strategies when simulations required re-adjustment of parameters.

These skills will serve as a foundation for future academic research and professional careers in photonics and optical communications.

7.3 Future Recommendations

While this project achieved its objectives, several opportunities remain for future work:

1. **Experimental Validation:**

- Fabricate Si_3N_4 PCFs and compare real-world performance with simulation results to validate confinement loss, dispersion, and SC bandwidth.

2. **Material and Structural Variations:**

- Explore hybrid PCF structures, such as **Si_3N_4 with oxide or chalcogenide claddings**, to extend operation into the mid-infrared region.
- Investigate PCFs with **mixed cladding geometries** (e.g., hybrid hexagonal + circular).

3. **Extended Wavelength Studies:**

- Perform SC simulations beyond $2\ \mu\text{m}$, targeting applications in **mid-IR spectroscopy and biomedical imaging** [28].

4. **Advanced Modeling:**

- Incorporate **Raman effects ($\text{fr} \neq 0$)** and **self-steepening terms** to capture additional nonlinear dynamics [28].
- Optimize for **pulse durations shorter than 50 fs**, which may yield even broader SC spectra.

By addressing these areas, future research can advance Si_3N_4 PCFs toward practical, high-performance broadband sources in optical networks, frequency metrology, and sensing platforms.

REFERENCES

- [1] S. Kaziz, F. Echouchene, and M. H. Gazzah, "Optimizing PCF-SPR sensor design through Taguchi approach, machine learning, and genetic algorithms," *Sci. Rep.*, vol. 14, no. 1, p. 7837, Apr. 2024, doi: 10.1038/s41598-024-55817-9.
- [2] C. Markos, J. C. Travers, A. Abdolvand, B. J. Eggleton, and O. Bang, "Hybrid photonic-crystal fiber," *Rev. Mod. Phys.*, vol. 89, no. 4, p. 045003, Nov. 2017, doi: 10.1103/RevModPhys.89.045003.
- [3] K. Ahmed, Md. S. Islam, and B. K. Paul, "Design and numerical analysis: Effect of core and cladding area on hybrid hexagonal microstructure optical fiber in environment pollution sensing applications," *Karbala Int. J. Mod. Sci.*, vol. 3, no. 1, pp. 29–38, Mar. 2017, doi: 10.1016/j.kijoms.2017.02.001.
- [4] G. Wang, G. Zeng, X. Cui, and S. Feng, "Dispersion analysis of the gradient weighted finite element method for acoustic problems in one, two, and three dimensions," *Int. J. Numer. Methods Eng.*, vol. 120, no. 4, pp. 473–497, Oct. 2019, doi: 10.1002/nme.6144.
- [5] R. R. Singh, D. Srivastava, W. Bhattacharya, N. Malviya, and A. Singh, "Performance analysis for mode confinement loss of photonic crystal fiber with circular air hole rings around the solid core," in *Micro-Structured and Specialty Optical Fibres VII*, C.-A. Bunge, K. Kalli, and P. Peterka, Eds., Strasbourg, France: SPIE, May 2022, p. 23. doi: 10.1117/12.2622204.
- [6] J. G. Porquez, R. A. Cole, and A. D. Slepko, "Comparison of two photonic crystal fibers for supercontinuum-Stokes spectral-focusing-CARS hyperspectroscopy," *OSA Contin.*, vol. 1, no. 4, p. 1385, Dec. 2018, doi: 10.1364/OSAC.1.001385.
- [7] S. Addanki, I. S. Amiri, and P. Yupapin, "Review of optical fibers-introduction and applications in fiber lasers," *Results Phys.*, vol. 10, pp. 743–750, Sept. 2018, doi: 10.1016/j.rinp.2018.07.028.
- [8] X. Wang, H. Yue, G. Liu, and Z. Zhao, "The Application of COMSOL Multiphysics in Direct Current Method Forward Modeling," *Procedia Earth Planet. Sci.*, vol. 3, pp. 266–272, 2011, doi: 10.1016/j.proeps.2011.09.093.
- [9] Md. E. Khan, S. Ben Khalifa, R. Amin, S. Chebaane, A. Dafhalla, and L. Manai, "A silicon nitride (Si₃N₄) filled PCF containing high birefringence and nonlinearity for optical applications," *Opt. Quantum Electron.*, vol. 56, no. 7, p. 1134, June 2024, doi: 10.1007/s11082-024-07066-3.

- [10] P. Russell, “Photonic Crystal Fibers,” *Science*, vol. 299, no. 5605, pp. 358–362, Jan. 2003, doi: 10.1126/science.1079280.
- [11] A. Frigg *et al.*, “Low loss CMOS-compatible silicon nitride photonics utilizing reactive sputtered thin films,” *Opt. Express*, vol. 27, no. 26, p. 37795, Dec. 2019, doi: 10.1364/OE.380758.
- [12] L. Wang *et al.*, “Frequency comb generation in the green using silicon nitride microresonators,” *Laser Photonics Rev.*, vol. 10, no. 4, pp. 631–638, July 2016, doi: 10.1002/lpor.201600006.
- [13] K. Saitoh and M. Koshiba, “Empirical relations for simple design of photonic crystal fibers,” *Opt. Express*, vol. 13, no. 1, p. 267, 2005, doi: 10.1364/OPEX.13.000267.
- [14] Y. D. Niu, D. N. Wang, Q. H. Wang, Z. K. Wang, and S. Qin Zhang, “Cascaded multiple Fabry–Perot interferometers fabricated in multimode fiber with a waveguide,” *Opt. Fiber Technol.*, vol. 58, p. 102306, Sept. 2020, doi: 10.1016/j.yofte.2020.102306.
- [15] S. Echeverri-Arteaga, H. Vinck-Posada, and E. A. Gómez, “The strange attraction phenomenon in cQED: The intermediate quantum coupling regime,” *Optik*, vol. 183, pp. 389–394, Apr. 2019, doi: 10.1016/j.ijleo.2019.02.032.
- [16] T. M. Monro, D. J. Richardson, N. G. R. Broderick, and P. J. Bennett, “Holey optical fibers: an efficient modal model,” *J. Light. Technol.*, vol. 17, no. 6, pp. 1093–1102, June 1999, doi: 10.1109/50.769313.
- [17] T. D. Bucio *et al.*, “Silicon Nitride Photonics for the Near-Infrared,” *IEEE J. Sel. Top. Quantum Electron.*, vol. 26, no. 2, pp. 1–13, Mar. 2020, doi: 10.1109/JSTQE.2019.2934127.
- [18] S. K. Pandey, S. Singh, and Y. K. Prajapati, “A novel PCF design with an ultra-flattened dispersion and low confinement loss by varying tiny air-hole concentration at core and cladding,” *Opt. Rev.*, vol. 28, no. 3, pp. 304–313, June 2021, doi: 10.1007/s10043-021-00662-8.
- [19] G. P. Agrawal, “Nonlinear Fiber Optics,” in *Nonlinear Science at the Dawn of the 21st Century*, vol. 542, P. L. Christiansen, M. P. Sørensen, and A. C. Scott, Eds., in Lecture Notes in Physics, vol. 542. , Berlin, Heidelberg: Springer Berlin Heidelberg, 2000, pp. 195–211. doi: 10.1007/3-540-46629-0_9.
- [20] J. Wang *et al.*, “Design and analysis for large-mode-area photonic crystal fiber with negative-curvature air ring,” *Opt. Fiber Technol.*, vol. 62, p. 102478, Mar. 2021, doi: 10.1016/j.yofte.2021.102478.

- [21] K. S. R. Atia, S. Ghosh, A. M. Heikal, M. F. O. Hameed, B. M. A. Rahman, and S. S. A. Obayya, "Finite Element Method for Sensing Applications," in *Computational Photonic Sensors*, M. F. O. Hameed and S. Obayya, Eds., Cham: Springer International Publishing, 2019, pp. 109–151. doi: 10.1007/978-3-319-76556-3_6.
- [22] J. M. Dudley, G. Genty, and S. Coen, "Supercontinuum generation in photonic crystal fiber," *Rev. Mod. Phys.*, vol. 78, no. 4, pp. 1135–1184, Oct. 2006, doi: 10.1103/RevModPhys.78.1135.
- [23] F. Poletti and P. Horak, "Description of ultrashort pulse propagation in multimode optical fibers," *J. Opt. Soc. Am. B*, vol. 25, no. 10, p. 1645, Oct. 2008, doi: 10.1364/JOSAB.25.001645.
- [24] H. Zia, "Simulation of white light generation and near light bullets using a novel numerical technique," *Commun. Nonlinear Sci. Numer. Simul.*, vol. 54, pp. 356–376, Jan. 2018, doi: 10.1016/j.cnsns.2017.05.033.
- [25] International Electrotechnical Commission, "IEC 60825-1 Safety of laser products—Part 1: Equipment classification and requirements," *Ed 30 IEC Geneva*, 2014.
- [26] E. ISO, "14644-1, 'Cleanrooms and associated controlled environments—Part 1: Classification of air cleanliness,'" *Eur. Stand.*, 1999.
- [27] M. Woods, M. Brown, M. Dabney, J. King, and G. Toncheva, "EVALUATION OF ANSI Z136. 1-2014 AND COMPARISON WITH Z136. 1-2007 AND ANSI Z136. 8-2012.," Sandia National Lab.(SNL-NM), Albuquerque, NM (United States), 2015.
- [28] R. Mukherjee and N. Borgohain, "Impact of self-steepening and intra-pulse Raman scattering on modulation instability in multiple quantum wells," *Eur. Phys. J. Plus*, vol. 138, no. 9, p. 867, Sept. 2023, doi: 10.1140/epjp/s13360-023-04509-w.

APPENDIX A
TURNITIN REPORT

Include here the 1st page of Turnitin Report

Every supervisor has his/her own Turnitin account. If not, then supervisors are requested to get the account from Library as soon as possible.

APPENDIX B

COMPLEX ENGINEERING PROBLEM SOLVING AND ENGINEERING ACTIVITIES

This appendix demonstrates how the undertaken project addressed **complex engineering problems (CEP)** and **complex engineering activities (CEA)** in accordance with BAETE outcome-based education (OBE) requirements.

B.1 Complex Engineering Problems (CEP) Solving

The project on **hexagonal Si₃N₄ photonic crystal fibers (PCFs)** involved addressing problems that meet the BAETE definition of complexity: requiring *in-depth engineering knowledge, analysis of multiple parameters, and trade-off evaluation*.

Attribute	Statement from this Project
P1 – Range of resources	Required advanced knowledge of photonics, nonlinear optics, and numerical simulation tools (COMSOL FEM, MATLAB GNLSE).
P2 – Level of interaction	Involved interaction of material properties (Si ₃ N ₄ refractive index), geometrical design (pitch, ratio, layers), and optical effects (dispersion, γ , CL).
P3 – Innovation	Designed novel 3-layer and 5-layer PCFs and compared their SC performance — a non-standard design problem requiring innovative geometry selection.
P4 – Consequences for society and environment	The findings can contribute to more efficient optical communication and sensing systems, impacting data transmission, healthcare, and metrology.
P5 – Familiarity	Required knowledge beyond routine coursework, including Sellmeier modeling, dispersion flattening, and nonlinear optics simulation.
P6 – Extent of stakeholder involvement and conflicting requirements	Trade-offs between confinement loss (low CL preferred by industry) and fabrication complexity (fewer layers easier to manufacture) had to be analyzed.
P7 – Interdependence	Demonstrated how changes in one parameter (e.g., pitch) influenced multiple outcomes (dispersion, γ , CL), requiring integrated optimization.

B.2 Complex Engineering Activities (CEA)

The project also meets the BAETE definition of complex engineering activities: involving the use of diverse tools, simulations, and evaluation across multiple criteria.

Attribute	Statement from this Project
Activity 1 – Design of solutions	Created and optimized PCF designs with multiple cladding layers to achieve desired dispersion and nonlinearity.
Activity 2 – Use of modern tools	Employed COMSOL Multiphysics for FEM simulations and MATLAB for solving the GNLSE.
Activity 3 – Depth of analysis	Analyzed multiple performance metrics (dispersion, CL, γ , SC spectra) under varying length and power conditions.
Activity 4 – Contextual knowledge	Considered real-world constraints such as fabrication complexity, optical communication standards, and energy efficiency.
Activity 5 – Teamwork and project management	Tasks were divided among group members (design, simulation, data analysis, report writing), improving teamwork and time management.

APPENDIX C

PROGRAM CODE

C.3 Code Listings

Complete Source Availability. To preserve readability, this appendix prints the main driver and essential function excerpts. The full, runnable MATLAB source (including main_sc_simulation.m, dispersion.m, gnlse.m, and README) is provided in Appendix_C_Code.zip and can be supplied to examiners on request.

C.3.1 Dispersion and beta

```
clc
clear all
close all
format long

c = 3e-7;           % Blue    p=5.5 ratio=0.12

del_lambda = 50*1e-12;
lambda = (950*1e-12:del_lambda:5050*1e-12);   % Unit of
wavelength (lambda) in km
N = length(lambda);
n_eff = [];

Beta02 = zeros(1,N);
for k = 2:N-1
    Beta02(k) = 1/(2*pi*c.^2)*lambda(k).^3*(n_eff(k+1)-
2*n_eff(k)+n_eff(k-1))/del_lambda^2;   % [Unit:ps^2/km]
end

D = zeros(1,N);
for k = 2:N-1
    D(k) = -2*1e-12*pi*c/lambda(k).^2*Beta02(k);   %
[Unit:ps/nm/km]
end

figure(1)
plot (lambda(2:N-1)/1e-9,D(2:N-
1),'linewidth',2,'Color','r');
%plot (lambda/1e-9,D);
xlabel ('Wavelength [\mum]');
ylabel ('D [ps/nm/km]');
hold on;
xline(1.55, 'b', 'linewidth', 0.5); % Vertical blue line at
X = 1.55
yline(0, 'b', 'linewidth', 0.5);   % Horizontal blue line
at Y = 0
hold off;
grid
```

```

%figure(2)
%plot (lambda(2:N-1)/1e-9,Beta02(2:N-1), 'linewidth',2, 'Color','r');
% %plot (lambda/1e-9,Beta2);
%xlabel ('Wavelength [\mum]');
%ylabel ('Beta2 [ps^2/km]');
%grid

```

C.3.2 Nonlinear coefficient and confinement loss

```

files = {};
colors = lines(length(files));
n2 = 2.4e-19;
line_styles = {'--',':', '-.', '-.'}; % For 4 Aeff curves, none solid

smooth_window = 7;

figure; clf;

%  $\gamma$  curves (solid lines, left y-axis)
yyaxis left;
hold on;
gamma_handles = [];
for i = 1:length(files)
    [~,~, raw] = xlsread(files{i});
    lambda_nm = cell2mat(raw(2:end,1));
    Aeff_um2 = cell2mat(raw(2:end,3));
    lambda_m = lambda_nm * 1e-9;
    Aeff_m2 = Aeff_um2 * 1e-12;
    gamma = (2 * pi ./ lambda_m) .* (n2 ./ Aeff_m2) * 1e3;
    gamma_smooth = smooth(gamma, smooth_window, 'moving');

    h = plot(lambda_nm, gamma_smooth, '-', 'LineWidth', 2, 'Color', colors(i,:));
    gamma_handles(end+1) = h;
end
ylabel('\gamma (W^{-1} km^{-1}));
xlabel('Wavelength (nm)');

% Aeff curves (dashed/dotted/dash-dot/solid, right y-axis)
yyaxis right;
hold on;
aeff_handles = [];
for i = 1:length(files)
    [~,~, raw] = xlsread(files{i});
    lambda_nm = cell2mat(raw(2:end,1));
    Aeff_um2 = cell2mat(raw(2:end,3));
    Aeff_smooth = smooth(Aeff_um2, smooth_window, 'moving');

```

```

    h = plot(lambda_nm, Aeff_smooth, line_styles{i}, 'LineWidth', 2.5, 'Color', colors(i,:));
    aeff_handles(end+1) = h;
end
ylabel('A_{eff} (\mum^2)');

legend([gamma_handles, aeff_handles], ...
    {'\gamma ', ...
    'A_{eff} '}, ...
    'Location', 'best');

title('Comparison of Nonlinear Coefficient and Effective Area');
grid on; box on;
hold off;

```

APPENDIX D
DATASHEET OF COMPONENTS